AIAA JOURNAL
Vol. 33, No. 3, March 1995

Substructure Synthesis Method for Frequency Response of Viscoelastic Structures

Duan Qian*
DeHavilland Inc., Downsview, Ontario M3K 1Y5, Canada
and
Jorn S. Hansen†
University of Toronto, Downsview, Ontario M3H 5T6, Canada

The method of substructure synthesis, previously applicable to undamped and viscously damped systems, has been extended to systems with viscoelastic damping in hereditary integral form, differential operator form and steady-state form. Based on a variational principle for symmetric systems, the corresponding substructure synthesis method is formulated in the frequency domain. Each substructure is represented by a set of admissible trial vectors in the Rayleigh–Ritz method. Eigenvectors of the corresponding undamped substructure and Ritz vectors obtained by spatial discretization of admissible functions are recommended as trial vectors. The traditional state-space formulation is avoided by the proposed substructure synthesis method so that the approach is independent of the form of viscoelastic models. The effectiveness of the proposed method in terms of reducing the size of final equations is illustrated through numerical examples.

Introduction

MODERN aerospace structures exhibit the characteristics of large size, light weight, and significant flexibility. Damping plays an important role to help stabilize control systems or to attenuate dynamic vibrations of these structures. The use of lightweight, high-strength composite materials may provide the passive damping desired. These materials are generally classified as viscoelastic. The finite element method reduces a continuous structure with complex geometry into a discrete system with a large number of degrees of freedom. The dynamic analysis of such a system is usually computationally expensive and sometimes impractical even with the capacity of current computers. The substructure synthesis method solves this problem by reducing a discrete system with a large number of degrees of freedom to another discrete system with a smaller number of degrees of freedom while still retaining the desired solution accuracy.

The main concept of approximating a substructure through the use of a set of trial vectors is common to all substructure synthesis methods. The required steps can be summarized as follows: 1) divide the structure into substructures, 2) represent the displacement of each substructure with a set of trial vectors, 3) couple the substructures by enforcing compatibility at their interfaces, 4) solve the reduced-size problem, and 5) transform the result back to the original system. Besides order reduction, substructure synthesis methods offer the following practical advantages: 1) independent design and analysis of various components of a structure by different contractors, 2) localized treatment of substructures with distinct properties such as viscoelasticity, 3) cost reduction for a re-analysis if not all of the substructures are modified, 4) simultaneous construction and reduction of substructural matrices on parallel computers, and 5) incorporation of experimental and analytical substructural characterization.

Substructure synthesis methods have been applied to the dynamic analysis of aerospace structures from the beginning of the space age to recent on-orbit structural load analysis of Space Station Freedom. Numerous substructure synthesis methods exist; most of these deal with the analysis of undamped structures. The most common approach is to use substructure modes as trial vectors; hence the term component mode synthesis. Based on conditions imposed at interfaces between one substructure and adjoining substructures, these methods can be further classified as fixed interface, free interface, and loaded interface. Hurty[1] developed the first component mode synthesis method using fixed interface modes, rigid-body modes, and redundant constraint modes as trial vectors. Craig and Bampton[2] simplified Hurty's method by pointing out that it is unnecessary to separate the set of constraint modes into rigid-body modes and redundant constraint modes. The original free interface method proposed by Goldman[3] has difficulty in representing local flexibility at interface points; the result is slow convergence. MacNeal[4] and Rubin[5] developed residual flexibility techniques to include the static effects of truncated higher order modes. Craig and Chang[6] identified Rubin's method as a consistent Ritz transformation using free interface modes and attachment modes as trial vectors. With the intention to find a set of substructure modes bearing some resemblance to the system modes, Gladwell[7] proposed a loaded interface method to include rigid-body inertia loading on a substructure due to the substructures connected to it. Benfield and Hruda[8] generalized the method by also applying the stiffness loading. The major drawbacks of this approach are the complexity of its implementation and the dependency of the data from other substructures. On the basis of the Rayleigh–Ritz approach, Meirovitch and Hale[9] proposed to represent each substructure with a suitable set of admissible vectors, which can be generated through spatial discretization of simple admissible functions. Other trial vectors, such as Lanczos vectors, were also considered in the literature. The starting vectors for Lanczos recurrence relationships were obtained as the static response due to either the actual load on the substructure[10] or some fictitious loads at substructure interfaces.[11]

The treatment for systems with proportional viscous damping is not so different from the treatment for undamped systems since the substructure modes of a damped system are the same as those of the associated undamped system. Nonproportional viscous damping is traditionally accommodated by a state-space formulation leading to complex substructure modes. Hasselman and Kaplan[12] extended Craig and Bampton's method[2] by using fixed interface complex substructure modes. Wu and Greif[13] devised a synthesis method using two successive transformations based upon consecutive use of free interface undamped modes in the physical coordinates followed by fixed interface damped complex modes in general coordinates. As an extension of Goldman's method,[3] Craig and Chung[14] used free interface complex modes in the mode synthesis. The method of supplementing the free interface complex modes with various complex attachment modes in improving convergence was also explored.[15,16]

Received July 28, 1993; revision received Jan. 24, 1994; accepted for publication May 5, 1994.

*Structural Dynamics Engineer.

†Professor, Institute for Aerospace Studies.

A substructure synthesis applicable to nonsymmetric systems was formulated by Craig and Ni[17] using both left and right free interface complex eigenvectors and attachment modes to form the left and right substructure transformation matrices, respectively. The complex conjugate transpose of the matrix of complex modes, instead of the traditional simple transpose, was proposed for the transformation in both the fixed[18] and free[19] interface method; thus the eigenvalues of the coupled structural system occur in complex conjugate pairs. The real and imaginary components of complex substructure eigenvectors can be used separately as trial vectors to obtain real matrices,[20] but they are no longer eigenvectors. According to Huston et al.,[21] there is little difference in the resulting eigen-solution whether complex substructure modes or real normal modes are used, even for cases with heavy damping and appreciably complex modes. Based on a variational principle in state space, Hale[22] formulated a substructure synthesis method for nonsymmetric systems. The displacement and velocity were represented independently in terms of real substructure admissible vectors, and interface compatibility was applied to both the displacement and velocity. A more extensive review on this subject is available in Ref. 23.

In this paper, the method of substructure synthesis, previously applicable to undamped and viscously damped systems, has been extended to systems with viscoelastic damping in hereditary integral form, differential operator form, and steady-state form. The solution of the frequency domain response can be made through a Fourier transform of the reduced motion equations in the time domain if the transform of the viscoelastic constitutive relations exists. However, not all viscoelastic damping models can be written in hereditary integral form. Based on a variational principle for symmetric systems, the proposed substructure synthesis method is formulated in the frequency domain. The traditional state-space formulation for systems with viscous damping is avoided in the present approach. Such a formulation is undesirable for systems with general viscoelastic damping for the following reasons. First, state-space formulations depend on the form of viscoelastic damping, which makes a computerized unified approach very difficult. Second, the size of state-space substructure equations increases with the number of viscoelastic constants used in the model when order reduction is needed in the first place. In addition, Ritz expansions for the newly introduced state variables are required, and geometric compatibility between substructures has also to be treated for the new variables. With the proposed method, each substructure is represented by a set of admissible trial vectors on the basis of the Rayleigh–Ritz approach. Variations of the method can be derived by using different types of trial vectors. Among them, eigenvectors of the corresponding undamped substructures with fixed or free interfaces and Ritz vectors obtained by spatial discretization of admissible functions are recommended. The approach is independent of the form of viscoelastic damping models, and the effort spent on the reduction process is similar to that in the classic component mode synthesis for undamped systems. In the absence of damping, the present method is identical to the classical method.

In the following sections, the types of viscoelastic constitutive relations applicable to the proposed substructure synthesis method are presented and summarized. Then a set of discrete motion equations of a viscoelastic structure is introduced, and its equivalent variational principle is developed. Based on a variational principle and the Rayleigh–Ritz approach, a substructure synthesis method is formulated. The selection of Ritz trial vectors is discussed. Finally, the effectiveness of the proposed method is illustrated through numerical examples.

Viscoelastic Constitutive Relations

Hereditary Integral Form

Based on the hypothesis that the local stress history is completely determined by the strain history and the restriction of linearity, continuity, causality, and translation invariance in time, an integral representation can be deduced for the most general linear hereditary stress-strain law[24]

$$\sigma_{ij}(t) = E_{ijkl}\,\epsilon_{kl}(t) + G_{ijkl}(t)\,\epsilon_{kl}(0) + \int_0^t G_{ijkl}(t-\tau)\,\dot{\epsilon}_{kl}(\tau)\,\mathrm{d}\tau \tag{1}$$

where $G_{ijkl}(t)$ is termed the relaxation function and $G_{ijkl}(\infty) = 0$. The Fourier transform of Eq. (1) yields

$$\bar{\sigma}_{ij}(\omega) = [E_{ijkl} + j\omega G_{ijkl}(\omega)]\,\bar{\epsilon}_{kl}(\omega) \tag{2}$$

The time-dependent function $G_{ijkl}(t)$ is usually expressed as a series of exponentials,[25]

$$G_{ijkl}(t) = \sum_{s=1}^{n} G_{ijkl}^{(s)}\,e^{-\theta_s t} \tag{3}$$

The problem of requiring a large number of relaxation coefficients to describe a viscoelastic material prompts a representation of relaxation functions with a continuous distribution,[26]

$$G_{ijkl}(t) = \int_0^\infty G_{ijkl}^{(0)}(\theta)\,\gamma(\theta)\,e^{-\theta t}\,\mathrm{d}\theta \tag{4}$$

Differential Operator Form

Standard linear viscoelastic models relate a series of time derivatives of the stresses to a series of time derivatives of strains. In one dimension, as suggested by Bland and Lee,[27] this becomes

$$\sum_{s=0}^{n_b} b_s D^s \sigma(t) = \sum_{s=0}^{n_a} a_s D^s \epsilon(t) \tag{5}$$

where the time operator is

$$D^s x(t) = \frac{\mathrm{d}^s x}{\mathrm{d}t^s} \tag{6}$$

Taking the Fourier transform of Eq. (5) under the assumption of zero initial stress and strain yields

$$\sum_{s=0}^{n_b} b_s (j\omega)^s\,\bar{\sigma}(j\omega) = \sum_{s=0}^{n_a} a_s (j\omega)^s\,\bar{\epsilon}(j\omega) \tag{7}$$

One of the special cases of this form is the classic Kelvin–Voigt model

$$\sigma(t) = E\,\epsilon(t) + C\,\dot{\epsilon}(t) \tag{8}$$

An alternative approach of modeling viscoelastic behavior is to use fractional derivatives. The general form of the fractional derivative model[28] is

$$b_0\,\sigma(t) + \sum_{s=1}^{n_b} b_s\,D^{\beta_s}\sigma(t) = a_0\,\epsilon(t) + \sum_{s=1}^{n_a} a_s\,D^{\alpha_s}\epsilon(t) \tag{9}$$

where the fractional derivative is defined by

$$D^\alpha x(t) = \frac{1}{\Gamma(1-\alpha)}\frac{\mathrm{d}}{\mathrm{d}t}\int_0^t \frac{x(\tau)}{(t-\tau)^\alpha}\,\mathrm{d}\tau, \qquad 0 < \alpha < 1 \tag{10}$$

Taking the Fourier transform of Eq. (9) with the properties of the transform of fractional derivatives yields

$$b_0\bar{\sigma}(\omega) + \sum_{s=1}^{n_b} b_s\,(j\omega)^{\beta_s}\bar{\sigma}(\omega) = a_0\bar{\epsilon}(\omega) + \sum_{s=1}^{n_a} a_s\,(j\omega)^{\alpha_s}\bar{\epsilon}(\omega) \tag{11}$$

According to Bagley and Torvik,[28] many viscoelastic materials can be modeled by retaining only the first term in each series.

Steady-State Form

If the applied load varies sinusoidally with time, the viscoelastic body may be assumed in a steady-state harmonic oscillation. Under this condition, the stress and strain histories are specified as being harmonic functions of time

$$\sigma(t) = \sigma_0(\omega)\, e^{j\omega t}, \qquad \epsilon(t) = \epsilon_0(\omega)\, e^{j\omega t} \tag{12}$$

A frequency-dependent complex modulus may be used to relate the steady-state stress σ_0 and strain ϵ_0

$$\sigma_0(\omega) = G^0(\omega)\, \epsilon_0(\omega) \tag{13}$$

The complex modulus $G^0(\omega)$ can be obtained directly from a sinusoidal test. This approach is motivated by the observation that the sinusoidal strain lags the sinusoidal stress by some phase angle. The commonly used hysteretic damping model is a special case of Eq. (13) wherein

$$G^0(\omega) = E + jH \tag{14}$$

The attractive feature of this model is its simplicity; however, it is inconsistent in the time domain due to the violation of causality.

General Form

The general form of the constitutive relations in the frequency domain are

$$\bar{\sigma}_{ij}(\omega) = [G'_{ijkl}(\omega) + jG''_{ijkl}(\omega)]\, \bar{\epsilon}_{kl}(\omega) \tag{15}$$

where the real functions $G'_{ijkl}(\omega)$ and $G''_{ijkl}(\omega)$ are usually referred to as the storage and loss moduli, respectively. Equation (15) includes the hereditary integral form (2), the differential operator forms (7) and (11), and the steady-state form (13).

Motion Equations

With the general form of the constitutive relations, Eq. (15), the following discretized motion equations can be obtained by applying the finite element method to a viscoelastic structure

$$(-\omega^2 \boldsymbol{M} + j\boldsymbol{K}'' + \boldsymbol{K}')\bar{\boldsymbol{U}} = \bar{\boldsymbol{F}} \tag{16}$$

where matrices $\boldsymbol{M}$, $\boldsymbol{K}'(\omega)$, and $\boldsymbol{K}''(\omega)$ are all symmetric; $\boldsymbol{M}$ is the mass matrix, whereas matrices $\boldsymbol{K}'(\omega)$ and $\boldsymbol{K}''(\omega)$ are related to the storage moduli $G'_{ijkl}(\omega)$ and loss moduli $G''_{ijkl}(\omega)$, respectively. According to the elastic-viscoelastic correspondence principle, they can be conveniently derived from the stiffness matrix of fully elastic elements when the appropriate frequency dependence is included. The displacement vector $\bar{\boldsymbol{U}}$ contains generalized displacements at the nodes, and the force vector $\bar{\boldsymbol{F}}$ represents the effect of external forces on the structure.

For hysteretic damping, in the light of Eq. (14), the matrix functions $\boldsymbol{K}'(\omega)$ and $\boldsymbol{K}''(\omega)$ reduce to constants, and Eq. (16) becomes

$$(-\omega^2 \boldsymbol{M} + j\boldsymbol{H} + \boldsymbol{K})\bar{\boldsymbol{U}} = \bar{\boldsymbol{F}} \tag{17}$$

A variational principle provides an equivalent form of the motion equations and a foundation for the substructure synthesis method. In this case, a bilinear functional can be conveniently introduced as

$$\Pi = \tfrac{1}{2}\langle(-\omega^2 \boldsymbol{M} + j\boldsymbol{K}'' + \boldsymbol{K}')\bar{\boldsymbol{U}}, \bar{\boldsymbol{U}}\rangle - \langle\bar{\boldsymbol{F}}, \bar{\boldsymbol{U}}\rangle \tag{18}$$

such that the motion equation (16) is given by the stationary condition $\delta\Pi = 0$, with the bilinear form of two vector functions $\bar{\boldsymbol{x}}(\omega)$ and $\bar{\boldsymbol{y}}(\omega)$ defined as

$$\langle\bar{\boldsymbol{x}}, \bar{\boldsymbol{y}}\rangle = \bar{\boldsymbol{x}}^T \bar{\boldsymbol{y}} \tag{19}$$

To prove this statement, the first variation of Π needs to be considered. This is given by

$$\begin{aligned}\delta\Pi = {}& \tfrac{1}{2}\langle(-\omega^2 \boldsymbol{M} + j\boldsymbol{K}'' + \boldsymbol{K}')\delta\bar{\boldsymbol{U}}, \bar{\boldsymbol{U}}\rangle \\ & + \tfrac{1}{2}\langle(-\omega^2 \boldsymbol{M} + j\boldsymbol{K}'' + \boldsymbol{K}')\bar{\boldsymbol{U}}, \delta\bar{\boldsymbol{U}}\rangle - \langle\bar{\boldsymbol{F}}, \delta\bar{\boldsymbol{U}}\rangle\end{aligned} \tag{20}$$

The symmetry of matrices $\boldsymbol{M}$, $\boldsymbol{K}'$, and $\boldsymbol{K}''$ results in

$$\langle(-\omega^2 \boldsymbol{M} + j\boldsymbol{K}'' + \boldsymbol{K}')\bar{\boldsymbol{x}}, \bar{\boldsymbol{y}}\rangle = \langle(-\omega^2 \boldsymbol{M} + j\boldsymbol{K}'' + \boldsymbol{K}')\bar{\boldsymbol{y}}, \bar{\boldsymbol{x}}\rangle \tag{21}$$

Applying the previous property (21), Eq. (20) becomes

$$\delta\Pi = \langle(-\omega^2 \boldsymbol{M} + j\boldsymbol{K}'' + \boldsymbol{K}')\bar{\boldsymbol{U}} - \bar{\boldsymbol{F}}, \delta\bar{\boldsymbol{U}}\rangle \tag{22}$$

We observe immediately that the Euler equation of the bilinear functional Π,

$$(-\omega^2 \boldsymbol{M} + j\boldsymbol{K}'' + \boldsymbol{K}')\bar{\boldsymbol{U}} - \bar{\boldsymbol{F}} = 0 \tag{23}$$

is identical to the original motion equation (16).

Substructure Synthesis

Assume that the structure is divided into N substructures. For a single substructure s, the motion satisfies N_s simultaneous equations in the frequency domain

$$\left(-\omega^2 \boldsymbol{M}_s + j\boldsymbol{K}''_s + \boldsymbol{K}'_s\right)\bar{\boldsymbol{U}}_s = \bar{\boldsymbol{F}}_s, \qquad s = 1, \ldots, N \tag{24}$$

Substructure matrices $\boldsymbol{M}_s$, $\boldsymbol{K}'_s(\omega)$, and $\boldsymbol{K}''_s(\omega)$ are symmetric; $\bar{\boldsymbol{U}}_s$ is the generalized substructure displacement vector. The generalized force vector $\bar{\boldsymbol{F}}_s$ consists of the sum of two parts, namely, a vector $\bar{\boldsymbol{F}}_{E_s}$ of external forces acting on substructure s and a vector $\bar{\boldsymbol{F}}_{I_s}$ of forces exerted on the internal boundaries B_{rs} of substructure s by all of the substructures r ($r = 1, \ldots, N$, $r \neq s$). Thus

$$\bar{\boldsymbol{F}}_s = \bar{\boldsymbol{F}}_{E_s} + \bar{\boldsymbol{F}}_{I_s}, \qquad s = 1, \ldots, N \tag{25}$$

Based on the variational principle, Eqs. (24) can be obtained as the conditions for the first variation of the following bilinear functional with respect to $\bar{\boldsymbol{U}}_s$ to vanish

$$\begin{aligned}\Pi_s = {}& \tfrac{1}{2}\left\langle\left(-\omega^2 \boldsymbol{M}_s + j\boldsymbol{K}''_s + \boldsymbol{K}'_s\right)\bar{\boldsymbol{U}}_s, \bar{\boldsymbol{U}}_s\right\rangle \\ & - \left\langle\bar{\boldsymbol{F}}_{E_s} + \bar{\boldsymbol{F}}_{I_s}, \bar{\boldsymbol{U}}_s\right\rangle, s = 1, \ldots, N\end{aligned} \tag{26}$$

The N substructures are now considered to act together so as to form the complete system. The motion equations are then given by the stationarity condition $\delta\Pi = 0$ with

$$\Pi = \sum_{s=1}^{N} \Pi_s \tag{27}$$

when the constraints are imposed in the form of internal boundary compatibility conditions between adjacent substructures. According to the force equilibrium conditions on internal boundary B_{rs} shared by substructures s and r, the force $\bar{\boldsymbol{F}}_{I_r}|_{B_{rs}}$ exerted by substructure s on substructure r must be equal in magnitude and opposite in direction to the force $\bar{\boldsymbol{F}}_{I_s}|_{B_{rs}}$ exerted by substructure r on substructure s. Thus

$$\bar{\boldsymbol{F}}_{I_s}|_{B_{rs}} = -\bar{\boldsymbol{F}}_{I_r}|_{B_{rs}} = \bar{\boldsymbol{F}}_{rs}, \qquad r, s = 1, \ldots, N, r \neq s \tag{28}$$

Inter-substructure force vector $\boldsymbol{F}_{rs}$ is assumed to be L_{rs} dimensional; $L_{rs} = 0$ if substructures r and s do not share a common boundary. Applying Eq. (28), Π can be written as

$$\begin{aligned}\Pi = {}& \sum_{s=1}^{N}\left\{\tfrac{1}{2}\left\langle\left(-\omega^2 \boldsymbol{M}_s + j\boldsymbol{K}''_s + \boldsymbol{K}'_s\right)\bar{\boldsymbol{U}}_s, \bar{\boldsymbol{U}}_s\right\rangle - \left\langle\bar{\boldsymbol{F}}_{E_s}, \bar{\boldsymbol{U}}_s\right\rangle\right\} \\ & - \sum_{s=1}^{N}\sum_{r=s+1}^{N}\left\langle\bar{\boldsymbol{U}}_s|_{B_{rs}} - \bar{\boldsymbol{U}}_r|_{B_{rs}}, \bar{\boldsymbol{F}}_{rs}\right\rangle\end{aligned} \tag{29}$$

It is now assumed that the number of degrees of freedom N_s for each substructure is large enough that a reduction is required. Based on the concept of the Rayleigh–Ritz method, the generalized displacement vector $\bar{\boldsymbol{U}}_s$ of each substructure s can be approximately represented by the sum of n_s trial vectors ϕ_{si} multiplying ω-dependent unknown coefficients $\bar{u}_{si}$

$$\bar{\boldsymbol{U}}_s(\omega) = \sum_{i=1}^{n_s} \phi_{si}\bar{u}_{si}(\omega) = \boldsymbol{\Phi}_s \bar{\boldsymbol{u}}_s(\omega), \qquad s = 1, \ldots, N \tag{30}$$

With $n_s \le N_s$, vector $\boldsymbol{u}_s$ is the n_s-dimensional unknown, and matrix $\boldsymbol{\Phi}_s$ contains n_s trial vectors ϕ_{si}. The trial vectors are required to be linearly independent and satisfy the external geometric boundary conditions of the whole structure. The concept of trial vectors for a substructure is analogous to that of the trial functions in the finite element model. Since the generalized displacement vector is complex in the frequency domain, complex trial vectors can be used in the expansion. Introducing Eq. (30) into Eq. (29) yields

$$\Pi = \sum_{s=1}^{N} \left\{ \tfrac{1}{2}\left\langle \left(-\omega^2 \boldsymbol{m}_s + jk_s'' + k_s'\right)\bar{\boldsymbol{u}}_s, \bar{\boldsymbol{u}}_s \right\rangle - \left\langle \bar{\boldsymbol{f}}_{E_s}, \bar{\boldsymbol{u}}_s \right\rangle \right\}$$

$$- \sum_{s=1}^{N} \sum_{r=s+1}^{N} \left\langle (\boldsymbol{\Phi}_s \bar{\boldsymbol{u}}_s)|_{B_{rs}} - (\boldsymbol{\Phi}_r \bar{\boldsymbol{u}}_r)|_{B_{rs}}, \bar{\boldsymbol{F}}_{rs} \right\rangle \tag{31}$$

where the $n_s \times n_s$ reduced substructure matrices are

$$\boldsymbol{m}_s = \boldsymbol{\Phi}_s^T \boldsymbol{M}_s \boldsymbol{\Phi}_s, \qquad \boldsymbol{k}_s'(\omega) = \boldsymbol{\Phi}_s^T \boldsymbol{K}_s'(\omega) \boldsymbol{\Phi}_s$$

$$\boldsymbol{k}_s''(\omega) = \boldsymbol{\Phi}_s^T \boldsymbol{K}_s''(\omega) \boldsymbol{\Phi}_s$$

and the n_s-dimensional reduced substructure external force vector is

$$\bar{\boldsymbol{f}}_{E_s} = \boldsymbol{\Phi}_s^T \bar{\boldsymbol{F}}_{E_s}, \qquad s = 1, \ldots, N$$

Rewriting Eq. (31) in block-diagonal assembled matrix form, we have

$$\Pi = \tfrac{1}{2}\left\langle \left(-\omega^2 \boldsymbol{m}_a + jk_a'' + k_a'\right)\bar{\boldsymbol{u}}_a, \bar{\boldsymbol{u}}_a \right\rangle$$

$$- \left\langle \bar{\boldsymbol{f}}_{E_a}, \bar{\boldsymbol{u}}_a \right\rangle - \left\langle \boldsymbol{C}_a \bar{\boldsymbol{u}}_a, \bar{\boldsymbol{F}}_{I_a} \right\rangle \tag{32}$$

where, with $n_a = \sum_{s=1}^{N} n_s$, the $n_a \times n_a$ block-diagonal matrices are

$$\boldsymbol{m}_a = \text{blk-diag}\, \boldsymbol{m}_s, \qquad \boldsymbol{k}_a'(\omega) = \text{blk-diag}\, \boldsymbol{k}_s'(\omega)$$

$$\boldsymbol{k}_a''(\omega) = \text{blk-diag}\, \boldsymbol{k}_s''(\omega)$$

and the n_a-dimensional disjoint vectors are

$$\bar{\boldsymbol{u}}_a = \left\{ \bar{\boldsymbol{u}}_1^T, \ldots, \bar{\boldsymbol{u}}_m^T \right\}^T, \qquad \bar{\boldsymbol{f}}_{E_a} = \left\{ \bar{\boldsymbol{f}}_{E_1}^T, \ldots, \bar{\boldsymbol{f}}_{E_m}^T \right\}^T$$

The notation $\langle \boldsymbol{C}_a \bar{\boldsymbol{u}}_a, \bar{\boldsymbol{F}}_{I_a} \rangle$ is used here to represent the summation

$$\left\langle \boldsymbol{C}_a \bar{\boldsymbol{u}}_a, \bar{\boldsymbol{F}}_{I_a} \right\rangle = \sum_{s=1}^{N} \sum_{r=s+1}^{N} \left\langle (\boldsymbol{\Phi}_s \bar{\boldsymbol{u}}_s)|_{B_{rs}} - (\boldsymbol{\Phi}_r \bar{\boldsymbol{u}}_r)|_{B_{rs}}, \bar{\boldsymbol{F}}_{rs} \right\rangle \tag{33}$$

The L_a-dimensional vector $\bar{\boldsymbol{F}}_{I_a}$ is formed by concatenating all vectors $\bar{\boldsymbol{F}}_{rs}$, hence $L_a = \sum_{s=1}^{N} \sum_{r=s+1}^{N} L_{rs}$. It will soon be clear that the $L_a \times n_a$ matrix $\boldsymbol{C}_a$ couples the substructures.

To ensure the structural integrity of the assembled system, the geometric compatibility conditions are defined as

$$\bar{\boldsymbol{U}}_a|_{B_{rs}} - \bar{\boldsymbol{U}}_r|_{B_{rs}} = 0, \qquad r, s = 1, \ldots, N, \; r \ne s \tag{34}$$

Substituting Eq. (30) into Eq. (34) yields

$$(\boldsymbol{\Phi}_s \bar{\boldsymbol{u}}_s)|_{B_{rs}} - (\boldsymbol{\Phi}_r \bar{\boldsymbol{u}}_r)|_{B_{rs}} = 0, \qquad r, s = 1, \ldots, N, \; r \ne s \tag{35}$$

and using the notation in Eq. (33), the geometric compatibility conditions (34) may be written in a compact form

$$\boldsymbol{C}_a \bar{\boldsymbol{u}}_a = 0 \tag{36}$$

In situations when actual geometric compatibility conditions imposed on an interface between substructures cannot be conveniently met, an approximation with the weighted residual method may be applied. The L_{rs}-dimensional complex vectors $\bar{\boldsymbol{F}}_{rs}$ are represented approximately by the truncated sum of l_{rs} ($l_{rs} \le L_{rs}$) linearly independent weighting vectors ψ_{rsj} multiplying ω-dependent unknown coefficients $\bar{f}_{rsj}$ as follows:

$$\bar{\boldsymbol{F}}_{rs}(\omega) = \sum_{j=1}^{l_{rs}} \psi_{rsj} \bar{f}_{rsj}(\omega) = \boldsymbol{\Psi}_{rs} \bar{\boldsymbol{f}}_{rs}(\omega) \qquad r, s = 1, \ldots, N, \; r \ne s \tag{37}$$

With $l_{rs} \le L_{rs}$, vector $\bar{\boldsymbol{f}}_{rs}$ is l_{rs} dimensional, and matrix $\boldsymbol{\Psi}_{rs}$ contains l_{rs} vectors ψ_{rsi}. Since the internal force vector is complex in the frequency domain, complex weighting vectors can be used in the expansion.

Equation (34) is equivalent to requiring that

$$\left\langle \bar{\boldsymbol{U}}_s|_{B_{rs}} - \bar{\boldsymbol{U}}_r|_{B_{rs}}, \bar{\boldsymbol{F}}_{rs} \right\rangle = 0, \qquad r, s = 1, \ldots, N, \; r \ne s \tag{38}$$

be satisfied for all possible vectors $\bar{\boldsymbol{F}}_{rs}$. By substituting Eqs. (30) and (37) into Eq. (38), it may be concluded that the actual geometric conditions are satisfied approximately if

$$\boldsymbol{\Psi}_{rs}^T \left[(\boldsymbol{\Phi}_s \bar{\boldsymbol{u}}_s)|_{B_{rs}} - (\boldsymbol{\Phi}_r \bar{\boldsymbol{u}}_r)|_{B_{rs}} \right] = 0 \qquad r, s = 1, \ldots, N, \; r \ne s \tag{39}$$

Note that the compatibility conditions on B_{rs} can be satisfied exactly if we let $l_{rs} = L_{rs}$ when $L_{rs} \le \min(n_r, n_s)$ in Eq. (37). Assembling the constraint equations (39) for all internal boundaries of all substructures yields

$$\boldsymbol{\Psi}_a^T \boldsymbol{C}_a \bar{\boldsymbol{u}}_a = 0 \tag{40}$$

where matrix $\boldsymbol{\Psi}_a$ contains a total of $l_a = \sum_{s=1}^{N} \sum_{r=s+1}^{N} l_{rs}$ weighting vectors.

Now the disjoint generalized displacement vector $\bar{\boldsymbol{u}}_a$ can be related to a vector $\bar{\boldsymbol{u}}$ containing $n = n_a - l_a$ independent unknowns through an $n_a \times n$ transformation matrix $\boldsymbol{C}$:

$$\bar{\boldsymbol{u}}_a = \boldsymbol{C} \bar{\boldsymbol{u}} \tag{41}$$

If the exact geometric compatibility conditions (36) are applied, $n = n_a - L_a$. Finally, introducing Eq. (41) into Eq. (32) yields the bilinear function Π for the coupled structure

$$\Pi = \tfrac{1}{2}\langle(-\omega^2 \boldsymbol{m} + jk'' + k')\bar{\boldsymbol{u}}, \bar{\boldsymbol{u}}\rangle - \langle \bar{\boldsymbol{f}}, \bar{\boldsymbol{u}} \rangle \tag{42}$$

where the $n \times n$ coupled matrices are

$$\boldsymbol{m} = \boldsymbol{C}^T \boldsymbol{m}_a \boldsymbol{C}, \qquad \boldsymbol{k}'(\omega) = \boldsymbol{C}^T \boldsymbol{k}_a'(\omega) \boldsymbol{C}$$

$$\boldsymbol{k}''(\omega) = \boldsymbol{C}^T \boldsymbol{k}_a''(\omega) \boldsymbol{C}$$

and the n-dimensional coupled external force vector is

$$\bar{\boldsymbol{f}} = \boldsymbol{C}^T \bar{\boldsymbol{f}}_{E_a}$$

Since matrices $\boldsymbol{m}$, $\boldsymbol{k}'(\omega)$, and $\boldsymbol{k}''(\omega)$ are symmetric, the condition of stationarity $\delta\Pi = 0$ gives the motion equation

$$(-\omega^2 \boldsymbol{m} + jk' + k'')\bar{\boldsymbol{u}} = \bar{\boldsymbol{f}} \tag{43}$$

Selection of Trial Vectors

As mentioned earlier, substructure trial vectors must be linearly independent and must satisfy the external geometric boundary conditions. Theoretically (not numerically), these conditions guarantee the exact representation of the substructure when $n_s = N_s$. In addition, the trial vectors are also desired to have acceptably smooth shapes so that the dynamic response of the structure in the low-frequency range is accurately represented.

Since the generalized displacement vector is complex in the frequency domain, complex trial vectors are allowed. As the frequency domain response is obtained by solving a set of linear algebraic equations with complex coefficients at each frequency ω, complex trial vectors, such as eigenvectors of the damped substructure, can be used in the Ritz expansion without further complicating the final solution step. However, the matrix operation and storage in the intermediate steps of the substructure synthesis become more computationally expensive if a complex transformation is applied.

Substructure eigenvectors are obviously admissible vectors. Traditionally, the motion of each substructure is represented by a linear combination of its eigenvectors. To accommodate viscous damping, the size of the eigenequations doubles due to the state-space formulation; the eigenvectors are also complex. The complex substructure eigenvectors not onlys become more difficult to compute but also lead to complex reduced matrices. The introduction of more general viscoelastic damping adds further complications. To obtain the substructure eigenvectors, a substructural eigenvalue problem has to be defined in terms of a model of viscoelastic damping such that the coefficient matrices can be diagonalized. The task of finding the substructure eigensolutions can be more challenging than calculating the frequency response of the system.

By definition, admissible vectors of a viscoelastic substructure are also those of the corresponding fully elastic substructure and vice versa. Therefore, admissible vectors for undamped systems can also be used for damped systems. The fixed and free interface normal modes of undamped substructures qualify as admissible vectors for damped substructures. With the use of undamped substructure modes as trial vectors, the definition of substructure eigenproblems involving viscoelastic damping and the subsequent solution for complex eigenvectors are avoided. However, are undamped modes good enough to approximate damped substructures? It is known that undamped modes are very close to damped modes when the damping is small, but this is not generally true for high damping. However, numerical examples given in the next section show a reduction of the maximum relative error at resonance with an increase in damping when undamped modes are used, even though the damped mode shapes depart from the shapes of the corresponding undamped modes. This suggests that, with an increase in damping, the requirement for a set of accurate modes is reduced.

Some admissible vectors, such as Lanczos vectors and Ritz vectors, can be obtained without solving an eigenvalue problem. The generation of Lanczos vectors involves factorization of the substructural stiffness matrix and orthogonalization of vectors, which was claimed to be less expensive than the solution of eigenproblems. Admissible Ritz vectors represent a much larger class of vectors than the substructure eigenvectors. As presented in Ref. 9, a convenient way of constructing admissible vectors is discretizing admissible functions. Consider the original continuous substructure from which the present discretized substructure was obtained by the finite element method. Such a continuous substructure admits a set of admissible functions. These admissible functions satisfy the geometric boundary conditions at external boundaries. They are also linearly independent, sufficiently differentiable, and form a complete set of functions. A set of low-order polynomials or sinusoidal functions are examples of admissible functions. Then a set of admissible vectors can be constructed by discretizing, or "sampling" in space, the set of admissible functions. In an admissible vector, the nodal displacement components take the values of the admissible function at the sampling points, whereas the nodal rotation components take the values of the first derivative of the admissible function at these sampling points. This process guarantees that admissible vectors satisfy all necessary conditions and also have smooth shapes.

Numerical Examples

Consider a cantilevered beam that consists of two uniform sections with the same density 1 kg/m, Young's modulus 10^{11} N/m^2, and length 50 m with the different sectional geometries 1 m × 0.5 m and 0.5 m × 0.25 m as shown in Fig. 1. Since the natural frequencies of a uniform beam with length l, linear density ρ, and bending stiffness EI are proportional to $\sqrt{EI/\rho l^4}$, only the sectional geometry has to be varied in a parametric study. The beam is naturally divided into two substructures. The one-dimensional viscoelastic constitutive relation can be written as

$$\bar{\sigma} = [G'(\omega) + jG''(\omega)]\bar{\epsilon}(\omega) = [E + j\omega G(\omega)]\bar{\epsilon} \tag{44}$$

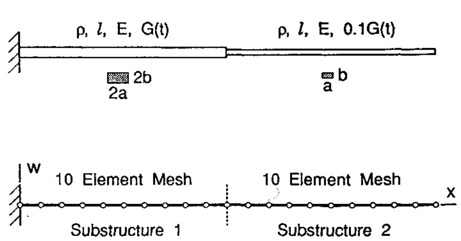

Fig. 1 Cantilevered beam model.

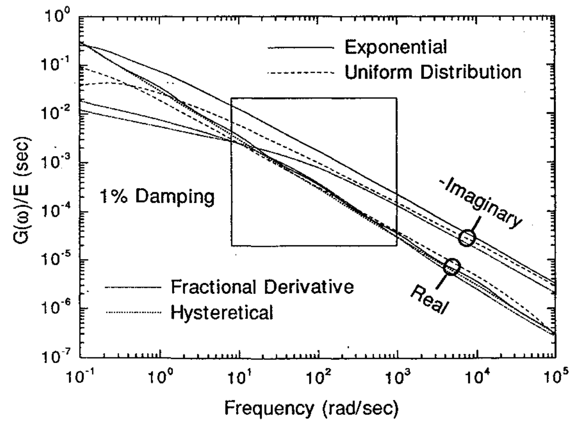

Fig. 2 Relaxation functions of various viscoelastic damping models.

For convenience, assume a relaxation function G in substructure 1 and 10% G in substructure 2. Four types of damping models are considered in the examples: the exponential damping model

$$G(\omega) = \sum_{k=1}^{7} \frac{5 \times 10^9}{j\omega + 10^{k-2}} \tag{45}$$

as a special case of both the hereditary integral form with discrete representation (3) and the standard linear viscoelastic model, the uniform distribution damping model

$$G(\omega) = \frac{1.26 \times 10^{14}}{10^5 - 10^{-1}} \int_{10^{-1}}^{10^5} \frac{\theta^{-0.9}}{j\omega - \theta} \, d\theta \tag{46}$$

as a special case of the hereditary integral form with continuous representation (4), the fractional derivative damping model

$$G(\omega) = \frac{5 \times 10^8}{j\omega} \frac{(j\omega)^{0.7} + (j\omega)^{0.6}}{1 + 0.1(j\omega)^{0.6}} \tag{47}$$

similar to Bagley and Torvik's five parameter model; and the hysteretic damping model

$$G(\omega) = \frac{3 \times 10^9}{\omega} \tag{48}$$

to represent a class of steady-state damping models that are valid in the frequency domain but not in the time domain. The parameters in all of the damping models are selected such that the first six equivalent damping factors η_e are approximately 1%, as shown in Table 1. The equivalent damping factor is related to the eigenvalue p_i by $\eta_e = -\mathrm{Re}(p_i)/\mathrm{Im}(p_i)$. The real and imaginary parts of the viscoelastic modulus $G(\omega)$ are plotted in Fig. 2 for the four types of damping modes.

A two-node cubic beam bending element is used to discretized the substructures. Two degrees of freedom are defined at each node: deflection w and slope dw/dx. Viscoelastic damping is incorporated into the elastic element by the correspondence principle at the element level. The full-sized discrete system is obtained by a mesh of 10 uniformly spaced elements in each substructure. Therefore, accounting for the two constraints, there are a total of 40 degrees of freedom in the coupled system. Then a reduced-order system of 20 degrees of freedom is obtained by the substructure synthesis method (SSM) with 10 trial vectors for substructure 1 and 12 for substructure 2.

Three types of trial vectors are considered here. 1) Discretized simple polynomials: the values of polynomial x^i and its slope ix^{i-1} at the coordinates of the nodal points are taken as the nodal values of displacement w and rotation dw/dx, respectively. Since substructure 1 is clamped at $x = 0$, external boundary conditions $w = 0$ and $dw/dx = 0$ can be satisfied by the choice of trial vectors. Hence, a sequence of x_i, $i = 2, 3, \ldots, 11$, is used for substructure 1 and a sequence of x_i, $i = 0, 1, \ldots, 11$, for substructure 2. 2) Fixed modes plus constraint modes: the first 8 and 10 lowest undamped normal modes are calculated for fixed-fixed substructure 1 and cantilevered

Table 1 Equivalent damping factors for various damping models

Mode no.	Natural frequency, 1/s	Equivalent damping factors, %: Exponential	Uniform distribution	Fractional derivative	Hysteretic
1	8.3602	0.92	0.67	0.64	0.84
2	31.480	0.79	0.73	0.92	0.82
3	88.525	1.24	1.17	1.47	1.24
4	183.52	0.88	0.94	1.05	0.91
5	274.60	0.88	1.02	1.05	0.97
6	426.71	1.11	1.33	1.23	1.25

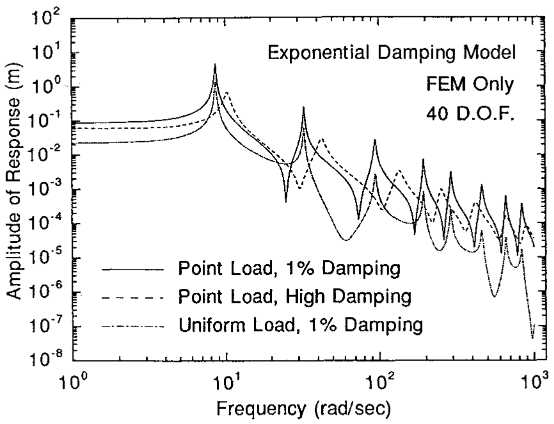

Fig. 3 Frequency response at the tip of the beam.

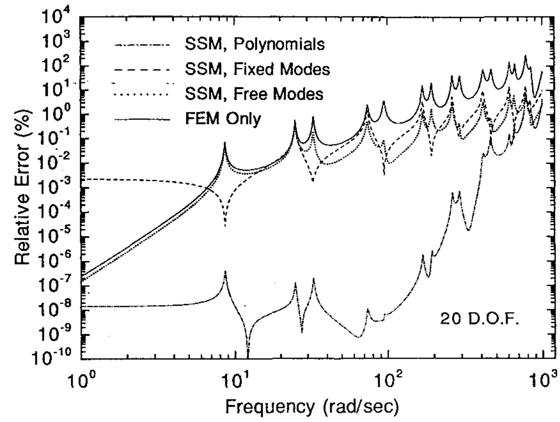

Fig. 4 Comparison of SSM and FEM at typical damping level with the exponential damping model; beam under point load.

substructure 2, respectively. Two constraint modes are obtained for each substructure by statically imposing a unit deflection and a unit rotation, respectively, at the internal boundary with the other freedom constrained. 3) The SSM with free modes plus attachment modes: the first 8 and 10 lowest undamped normal modes are calculated for cantilevered substructure 1 and unconstrained substructure 2, respectively. Two standard attachment modes are obtained for each substructure by statically imposing a unit force and a unit moment, respectively, at the unconstrained internal boundary degrees of freedom. Statically determinate constraints inhibiting rigid-body motion are applied at the other end of substructure 2. Since the proposed method is the only SSM for the frequency response of viscoelastic systems, a comparison with other SSM is not possible. Hence, the results are compared with those of a direct finite element approach without substructuring. A reduced-order system of 20 degrees of freedom was formed directly by the finite element method (FEM), using five equal elements in each section of the beam. The resulting sets of linear algebraic equations with complex coefficients were solved using the IMSL subroutine LEQT1C (Ref. 29) at each frequency. Frequency response of the displacement at the tip of the beam $\Delta(\omega)$ is chosen to monitor the error in the solution. The relative error between the approximate solution Δ^a, based on the reduced-order system, and the exact solution Δ^e, based on the full-sized system, is defined as

$$\frac{\|\Delta^a(\omega) - \Delta^e(\omega)\|}{\|\Delta^e(\omega)\|} \tag{49}$$

where the amplitude $\|\Delta\| = \sqrt{\mathrm{Re}^2(\Delta) + \mathrm{Im}^2(\Delta)}$.

Two separate loading cases are considered: a concentrated load of 100 N imposed at the tip of the beam and a uniformly distributed load of 1 N/m intensity over the entire beam. For completeness, the amplitude of frequency response of the full-sized system is given in Fig. 3 for both loading cases. The exponential damping mode is applied at two damping levels that have a factor of 10 difference in the relaxation function. Referring to Fig. 3, the absolute error of various solutions can be assessed based on the corresponding relative error.

The relative error of the SSM and the reduced FEM is compared in Fig. 4 for the point load case with the exponential damping model given by Eq. (45). In the sequence of twin peaks following the first peak, the first peak of a twin corresponds to a valley on the corresponding frequency response curve (point load, 1% damping) in Fig. 3. Therefore, the high relative error is the result of a small absolute error and a small denominator, which should not cause much concern. We shall focus our attention on the second peak of a twin, corresponding to a resonance peak of the frequency response in Fig. 3. The SSM with polynomials provides at least five more significant figures than the FEM up to the fourth natural frequency, then reduces to three at the sixth. This confirms the ability of low-order polynomials in representing arbitrary shapes of smooth, low-frequency modes. The SSM with free modes performs only slightly better than the FEM up to the second resonance frequency and provides one to two more significant figures in the high-frequency range. Its error rises slower than that of the FEM with increased frequency. The relative error curve of the SSM with fixed modes has a feature distinctively different from the others. It has a valley at the resonance frequency where the other methods produce a peak. This SSM provides a solution with two to three more significant figures in the neighborhood of the first six resonance frequencies.

The results for the uniform distribution damping model given by Eq. (46), the fractional derivative damping model given by Eq. (47), and the hysteretic damping model given by Eq. (48) are very similar to those for the exponential damping model in Fig. 4. The relative error for all four damping models is bounded between a pair of curves resulted from the exponential damping model and the hysteretic damping model. Therefore, for conciseness and clarity, only the two bounds of the relative error curves are shown in Fig. 5 for each variant of the SSM. It is clear that the type of viscoelastic damping model used in the analysis has little effect on the error introduced by the proposed SSM, if they represent similar viscoelastic characteristics, as shown by the relaxation functions in Fig. 2. The computational effort involved in the reduction process with the present SSM is also independent of the type of damping model.

To study the influence of damping level, the relaxation function of the exponential damping model is increased by a factor of 10. The relative error for high damping level is shown in Fig. 6. The peak relative error at resonance frequencies flattens out at high damping level for all types of trial vectors. So does the absolute error, based on the frequency response (point load, high damping) in Fig. 3.

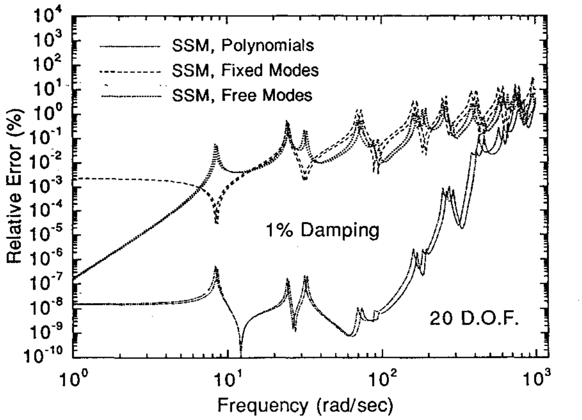

Fig. 5 Effect of the type of damping models on the relative error; beam under point load.

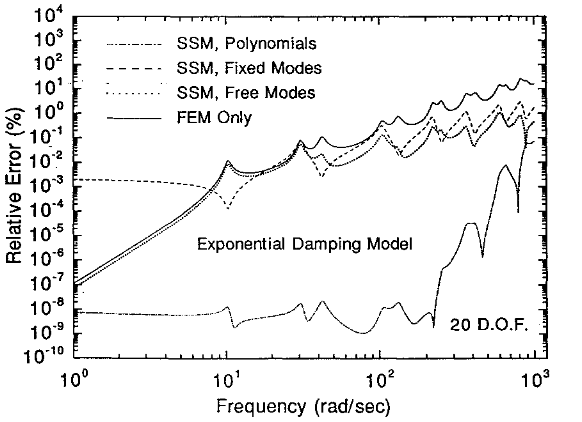

Fig. 6 Effect of higher damping level on the relative error; beam under point load.

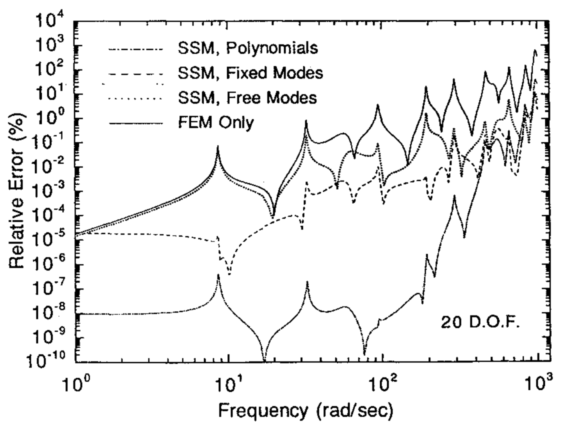

Fig. 7 Comparison of SSM and FEM at typical damping level with the exponential damping model; beam under uniform load.

Therefore high damping does not represent a challenge to the SSM with any type of trial vectors. Although undamped real modes do not resemble highly damped modes, the error introduced through the use of real modes in the forced response calculations of a highly damped system is not any larger than that of the corresponding lightly damped system.

As an alternative to the point load in the previous examples, the relative error for the uniform load case is shown in Fig. 7. Comparing Fig. 7 with Fig. 4, the relative error of the SSM with fixed modes is significantly reduced under the uniform load, whereas the peak relative error of the FEM and the SSM with other trial vectors is hardly affected by different loading conditions. The frequency response under uniform load in Fig. 3 has flat valleys between the resonance peaks, which no longer produce peaks on relative error plots.

Conclusions

A substructure synthesis method is developed in the frequency domain for structures with viscoelastic damping in hereditary integral form, differential operator form, and steady-state form. The method is an extension of the existing methods for structures with viscous damping. The formulation is based on a variational principle for symmetric viscoelastic systems. Because of the removal of the traditional state-space formulation within the substructure synthesis, the approach is independent of the form of the viscoelastic damping model, and the computational effort spent on the reduction process is similar to that in the classic component mode synthesis method for undamped systems.

On the basis of the Rayleigh–Ritz method, each substructure is represented by a set of admissible trial vectors. Although the complex eigenvectors of the viscoelastic substructure can be used as trial vectors, their use is neither necessary nor desirable. The complex eigenvectors are not easy to obtain and difficult to work with computationally. Real trial vectors are recommended. Eigenvectors and Lanczos vectors of the corresponding undamped substructure as well as Ritz vectors obtained by spatial discretization of simple functions are in this category. The first two types of admissible vectors depend on the geometry, mass, and stiffness properties, whereas the last one depends only on the geometry of the substructure. If the circumstance requires, the geometric compatibility conditions between substructures may be approximated by a weighted residual method.

Viscoelastic beam examples have been presented to illustrate the proposed substructure synthesis method. Examination of the results yields the following conclusions for these examples: 1) The proposed method is insensitive to the type of damping model, provided the models represent similar viscoelastic characteristics. 2) The use of undamped modes appears to be adequate in substructure synthesis of structures that contain even high levels of viscoelastic damping. 3) The use of normal modes of undamped substructures as trial vectors is capable of significantly improving the solution of viscoelastic systems, as compared with a direct finite element method without substructuring. 4) The trial vectors generated from simple polynomials yield remarkably good results in the low-frequency range.

References

[1]Hurty, W. C., "Dynamic Analysis of Structural Systems Using Component Modes," *AIAA Journal*, Vol. 3, No. 4, 1965, pp. 678–685.

[2]Craig, R. R., Jr., and Bampton, M. C. C., "Coupling of Substructures for Dynamic Analysis," *AIAA Journal*, Vol. 6, No. 7, 1968, pp. 1313–1319.

[3]Goldman, R. L., "Vibration Analysis by Dynamic Partitioning," *AIAA Journal*, Vol. 7, No. 6, 1969, pp. 1152–1154.

[4]MacNeal, R. H., "A Hybrid Method of Component Mode Synthesis," *Computers and Structures*, Vol. 1, No. 4, 1971, pp. 581–601.

[5]Rubin, S., "Improved Component-Mode Representation for Structural Dynamic Analysis," *AIAA Journal*, Vol. 13, No. 8, 1975, pp. 995–1006.

[6]Craig, R. R., Jr., and Chang, C. J., "On the Use of Attachment Modes in Substructural Coupling for Dynamic Analysis," *Proceedings of the AIAA/ASME/ASCE/AHS 18th Structures, Structural Dynamics, and Materials Conference* (San Diego, CA), AIAA, New York, 1977, pp. 89–99.

[7]Gladwell, G. M. L., "Branch Mode Analysis of Vibrating Systems," *Journal of Sound and Vibration*, Vol. 1, No. 1, 1964, pp. 41–59.

[8]Benfield, W. A., and Hruda, R. F., "Vibration Analysis of Structures by Component Mode Substitution," *AIAA Journal*, Vol. 9, No. 7, 1971, pp. 1255–1261.

[9]Meirovitch, L., and Hale, A. L., "On the Substructure Synthesis Method," *AIAA Journal*, Vol. 19, No. 7, 1981, pp. 940–947.

[10]Wilson, E. L., and Bayo, E. P., "Use of Special Ritz Vectors in Dynamic Substructure Analysis," *Journal of Structural Engineering*, Vol. 112, No. 8, 1986, pp. 1944–1956.

[11]Craig, R. R., Jr., and Hale, A. L., "Block-Krylov Component Synthesis Method for Structural Model Reduction," *Journal of Guidance, Control, and Dynamics*, Vol. 11, No. 6, 1988, pp. 562–570.

[12]Hasselman, T. K., and Kaplan, A., "Dynamic Analysis of Large Systems by Complex Mode Synthesis," *Journal of Dynamic Systems, Measurement and Control, Transactions of ASME*, Series G, Vol. 96, Sept. 1974, pp. 327–333.

[13]Wu, L., and Greif, R., "Substructuring and Modal Synthesis for Damped Systems," *Journal of Sound and Vibration*, Vol. 90, No. 3, 1983, pp. 407–422.

[14]Craig, R. R., Jr., and Chung, Y.-T., "Generalized Substructure Coupling Procedure for Damped Systems," *AIAA Journal*, Vol. 20, No. 3, 1982, pp. 442–444.

[15]Chung, Y.-T., and Craig, R. R., Jr., "State Vector Formulation of Substructure Coupling for Damped Systems," *Proceedings of the AIAA/ASME/ASCE/AHS 24th Structures, Structural Dynamics, and Materials Conference* (Lake Tahoe, NV), AIAA, New York, 1983, pp. 520–528.

[16]Howsman, T. G., and Craig, R. R., Jr., "A Substructure Coupling Procedure Applicable to General Linear Time-Invariant Dynamic Systems," *Proceedings of the AIAA/ASME/ASCE/AHS 25th Structures, Structural Dynamics, and Materials Conference* (Palm Springs, CA), AIAA, New York, 1984, pp. 164–171.

[17]Craig, R. R., Jr., and Ni, Z., "Component Mode Synthesis for Model Order Reduction of Nonclassically Damped Systems," *Journal of Guidance, Control, and Dynamics*, Vol. 12, No. 4, 1989, pp. 577–584.

[18]Béliveau, J.-G., and Soucy, Y., "Damping Synthesis Using Complex Substructure Modes and a Hermitian System Representation," *AIAA Journal*, Vol. 23, No. 12, 1985, pp. 1952–1956.

[19]Béliveau, J.-G., and Rong, H., "Damping Synthesis Using Residual Free Interface Inertial Relief Complex Attachment Modes," *Proceedings of the AIAA/ASME/ASCE/AHS/ASC 32nd Structures, Structural Dynamics, and Materials Conference* (Baltimore, MD), AIAA, Washington, DC, 1991, pp. 2472–2778.

[20]Kubomura, K., "Component Mode Synthesis for Damped Structures," *AIAA Journal*, Vol. 25, No. 5, 1987, pp. 740–745.

[21]Huston, D. R., Béliveau, J.-G., and Graves, W. R., "Experimental Verification of Complex Component Mode Synthesis," *Proceedings of the AIAA/ASME/ASCE/AHS/ASC 32nd Structures, Structural Dynamics, and Materials Conference* (Baltimore, MD), AIAA, Washington, DC, 1991, pp. 2441–2451.

[22]Hale, A. L., "Substructure Synthesis and Its Iterative Improvement for Large Nonconservative Vibratory Systems," *AIAA Journal*, Vol. 22, No. 2, 1984, pp. 265–272.

[23]Qian, D., "Substructure Synthesis Methods for Viscoelastic Structures," Ph.D. Thesis, Inst. for Aerospace Studies, Univ. of Toronto, Downsview, Ontario, Canada, 1993.

[24]Christensen, R. M., *Theory of Viscoelasticity*, Academic Press, New York, 1982.

[25]Staverman, A. J., and Schwarzl, F., "Non-Equilibrium Thermodynamics of Viscoelastic Behavior," *Koninklijke Nederlandse Akademic Van Wetenschappen, Proceeding of the Section of Sciences*, Series B, Vol. 55, 1952, pp. 486–492.

[26]Biot, M. A., "The Theory of Stress-Strain Relations in Anisotropic Viscoelasticity and Relaxation Phenomena," *Journal of Applied Physics*, Vol. 25, No. 11, 1954, pp. 1385–1391.

[27]Bland, D. R., and Lee, E. H., "Calculation of the Compliance Modulus of Linear Viscoelastic Materials from Vibrating Reed Measurements," *Journal of Applied Physics*, Vol. 26, No. 12, 1955, pp. 1497–1503.

[28]Bagley, R. L., and Torvik, P. J., "Fractional Calculus—A Different Approach to the Analysis of Viscoelastically Damped Structures," *AIAA Journal*, Vol. 21, No. 5, 1983, pp. 741–748.

[29]*The IMSL Library*, International Mathematical & Statistical Libraries, Inc., 1984.